Influence of CuO nanoparticles and nanographene platelets on the photosonocatalytic performance of Fe_3O_4/TiO_2 nanocomposites

M. Fauzian[1,2], F. F. Harno[1,2], A. Taufik[1,2], R. Saleh[1,2*]
[1]Departemen Fisika, Fakultas MIPA-Universitas Indonesia, 16424 Depok, Indonesia

[2]Integrated Laboratory of Energy and Environment, Fakultas MIPA-Universitas Indonesia, 16424 Depok, Indonesia

E-mail: rosari.saleh@ui.ac.id

Abstract. The effect of adding CuO nanoparticles and Nanographene Platelets (NGP) on Fe_3O_4/TiO_2 nanocomposites to degrade dye waste were examined using photosonocatalytic process. Both nanocomposites Fe_3O_4/TiO_2 with and without the addition of CuO were synthesized using sol-gel method, while the co-precipitation method was used to synthesize those two nanocomposites with NGP. All the samples were analyzed to identify their crystalline phase, magnetic property and thermal stability using X-Ray Diffraction (XRD), Vibrating Sample Magnetometer (VSM) and Thermogravimetric Analysis (TGA) measurements. The photosonocatalytic process of all samples were observed using the ultraviolet and ultrasonic radiation at the same time with the Methylene Blue (MB) as the model of dye waste. The results indicate that the presence of CuO nanoparticles and NGP on Fe_3O_4/TiO_2 nanocomposites could increase its capacibility to degrade MB. Achievement of degradation up to 100 % for a time of 2 hours is obtained by the presence of CuO nanoparticles and NGP simultaneously on Fe_3O_4/TiO_2 nanocomposites.

1. Introduction

Recently, dye waste water is easily found in the textile industry that cause a damage for the environment [1-3]. Therefore it is important to treat dye waste water from textile industry before discharge to the environment. Advance Oxidation Process (AOPs) is very promising in waste water treatment due to its ability to decompose dye waste water into the harmless molecules [4-5]. The AOPs methods that mostly used is photosonocatalytic which combines both photocatalytic and sonocatalytic process at the same time [6-8]. The use of photosonocatalytic process in waste water removal is reported to have better efficiency compared to photocatalytic and sonocatalytic process. This is because of the synergy effect between photocatalytic and sonocatalytic process [7].

Semiconductor materials have been commonly used in the AOPs process such as photocatalytic, sonocatalytic and photosonocatalytic process for waste water removal [8-10]. Titanium Oxide (TiO_2) is very promising materials in the AOPs process because this material is very cheap, environment friendly and active under the exposure of UV (ultraviolet) irradiation [11]. However, studies on the process of waste degradation using the AOPs process such as photosonocatalytic lead to use of material composite as the catalyst. The advantage of this material composite is the synergic effect of each material in the composite that can increase the efficiency of waste degradation through the photosonocatalytic process

[12-13]. The use of Fe_3O_4/TiO_2 nanocomposites have been reported to have better capacibility to degrade waste than the TiO_2 nanoparticle because the recombination rate of electron and hole in TiO_2 is inhibited by the presence of Fe_3O_4 [14].
In addition to Fe_3O_4, other materials which are promising to use with TiO_2 nanocomposites are CuO nanoparticles and carbon nanomaterials such as graphene. The advantage of CuO in the material composite as the catalyst is its ability to inhibit the recombination rate of electron and hole and its ability to extend the absorption toward visible region [15-17]. In addition to having the capacibility to inhibit the recombination rate of electron and hole, graphene also has the ability to expand the surface area of catalyst [18-19]. Therefore, in this study, we investigated the influence of addition of nanoparticles of CuO and Nanographene platelets (NGP) on the ability of Fe_3O_4/TiO_2 nanocomposites to degrade methylene blue (MB) wastes through the photosonocatalytic process.

2. Experimental

The materials used in the synthesis process are among others: Iron (II) sulfate heptahydrate ($FeSO_4.7H_2O$, 99%), copper sulfate pentahydrate ($CuSO_4.5H_2O$, 99%), titanium dioxide (TiO_2, 99%), sodium hydroxide (NaOH), ethanol, ethylene glycol (EG), and Nanographene Platelets (NGP). All the reagents used do not undergo further purification. Fe_3O_4/TiO_2 and $Fe_3O_4/CuO/TiO_2$ nanocomposites were synthesized under the method already reported in the previous studies [20]. Meanwhile the synthesis process of nanocomposites with NGP addition to Fe_3O_4/TiO_2 and $Fe_3O_4/CuO/TiO_2$ were performed using the co-precipitation method. The NGP was dispersed into the solution of distilled water and ethanol. This solution was afterward put into an ultrasonic bath at the frequency of 40 kHz for 2 hours. Then poured Fe_3O_4/TiO_2 (or $Fe_3O_4/CuO/TiO_2$) nanocomposites into the NGP solution and subsequently stirred the mixture using magnetic stirrer for 1 hour. Afterward, heated the mix at the temperature of 120^{o}C for 3 hours and dry up under vacuum condition for 12 hours.
The crystalline phase and structure of all samples were analyzed using X-Ray Diffraction (XRD) Rigaku Miniflex 600. The magnetic property of the samples were analyzed using Vibrating Sample Magnetometry (VSM) Oxford Type 1.2T. The thermal stability of the samples were analyzed using the Thermogravimetric Analysis (TGA) Rigaku TG/TGA 8121 measurement.
The photosonocatalytic activities of all samples were investigated by observing the degradation of *Methylene Blue* (MB) using ultrasonic bath operated at the frequency of 40 kHz and electrical power of 40 W with ultraviolet (UV) light irradiaton at the same time. First of all, catalyst is dispersed into a beaker containing MB solution with the concentration of 20 mg/L. Prior to the photosonocatalytic process, the solution was stirred with magnetic stirrer under dark condition for 30 minutes to reach the adsorption-desorption equilibrium. The pH of the solution was maintained at pH 13. The photosonocatalytic process were done for 2 hours and with the interval of every 15 minutes the MB solution was analyzed using UV-Vis Spectroscopy to observe the rate of MB degration before and after the process.

3. Results and discussion

Figure 1(a) shows the result of magnetic property measurement using VSM from the samples of Fe_3O_4 nanoparticles, Fe_3O_4/TiO_2, $Fe_3O_4/CuO/TiO_2$ and $Fe_3O_4/CuO/TiO_2$/NGP nanocomposites. The figure shows that all samples have the ferromagnetic hysteresis curves at room temperature. The magnetic saturation (M-S) of all samples are listed in Table 1. The M-S value of Fe_3O_4 is 82 emu/g, the addition of diamagnetic material of TiO_2 reduces the magnetization value to 65 emu/g. Furthermore, the reduction in magnetization value to 50 emu/g also occurs with the addition of anti-ferromagnetic material of CuO. However the opposite trend happens when NGP is added to $Fe_3O_4/CuO/TiO_2$ nanocomposites, its M-S value increases to 55 emu/g. The risen value in magnetic saturation may due to the stabilize state of Fe_3O_4 in the surface of NGP [21].

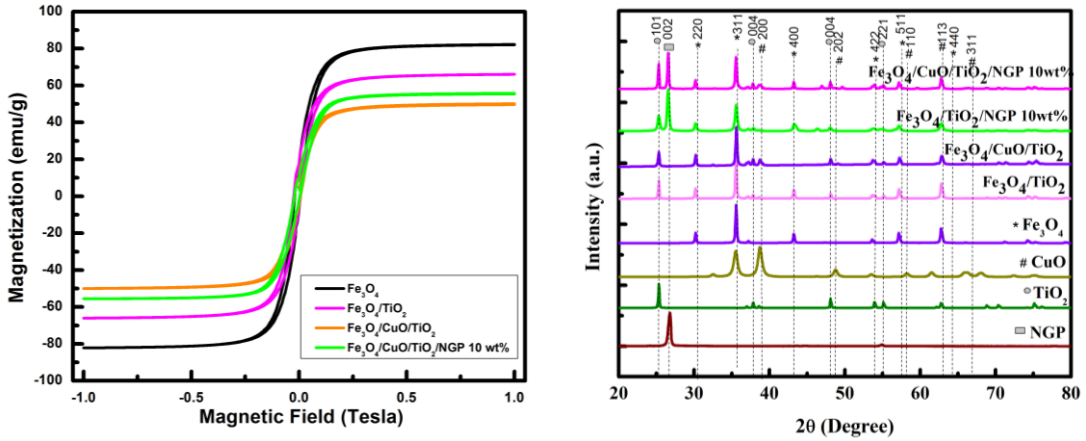

Figure 1. (a) Magnetic curve of pure Fe_3O_4, Fe_3O_4/TiO_2, $Fe_3O_4/CuO/TiO_2$, and $Fe_3O_4/CuO/TiO_2$/NGP 10 wt% nanocomposites, (b) XRD spectra of pure Fe_3O_4, TiO_2, CuO nanoparticles, NGP, Fe_3O_4/TiO_2, $Fe_3O_4/CuO/TiO_2$, Fe_3O_4/TiO_2/NGP and $Fe_3O_4/CuO/TiO_2$/NGP nanocomposites.

Figure 1(b) indicates the result of XRD measurement of the Fe_3O_4/TiO_2, $Fe_3O_4/CuO/TiO_2$, Fe_3O_4/TiO_2/NGP and $Fe_3O_4/CuO/TiO_2$/NGP nanocomposites. As comparison, we include the XRD curves from Fe_3O_4, CuO, and TiO_2 nanoparticles. By comparing the XRD curves, it can be seen that the main peaks in the Fe_3O_4/TiO_2 nanocomposite consists of the cubic spinel phase of Fe_3O_4 and anatase phase of TiO_2. For Fe_3O_4/TiO_2/NGP nanocomposites, there are cubic spinel phase of Fe_3O_4, anatase phase of TiO_2, and graphite-like structure of NGP. For $Fe_3O_4/CuO/TiO_2$ nanocomposite, there are monoclinic phase of CuO present in the XRD curve and also graphite-like structure of NGP for $Fe_3O_4/CuO/TiO_2$/NGP. The XRD curves of all samples confirm that the resulting nanocomposites are synthesized as desired.

TGA measurement from samples of Fe_3O_4/TiO_2, $Fe_3O_4/CuO/TiO_2$, Fe_3O_4/TiO_2/NGP and $Fe_3O_4/CuO/TiO_2$/NGP are shown in Figure 2(a). Both Fe_3O_4/TiO_2 and Fe_3O_4 /CuO/TiO_2 nanocomposites results do not indicate the significant percentage loss. It can be said that both of Fe_3O_4/TiO_2 and $Fe_3O_4/CuO/TiO_2$ nanocomposites are stable until temperature of 1000°C. With the presence of NGP, these nanocomposites have the percentage losses at the temperature of 600-1000°C. Such percentage loss occurs as a result of the combustion process of NGP materials inside these nanocomposites when the temperature is above 600 °C. Together with the XRD curves, TGA results also confirm the presence of NGP in the nanocomposites of Fe_3O_4/TiO_2/NGP and $Fe_3O_4/CuO/TiO_2$/NGP.

Table 1. Magnetic saturation of Fe_3O_4 nanoparticles, nanocomposites of Fe_3O_4/TiO_2, $Fe_3O_4/CuO/TiO_2$, and $Fe_3O_4/CuO/TiO_2$/NGP

Sample	Magnetic saturation
Fe_3O_4	82
Fe_3O_4/ TiO_2	65
$Fe_3O_4/CuO/TiO_2$	50
$Fe_3O_4/CuO/TiO_2$/NGP	55

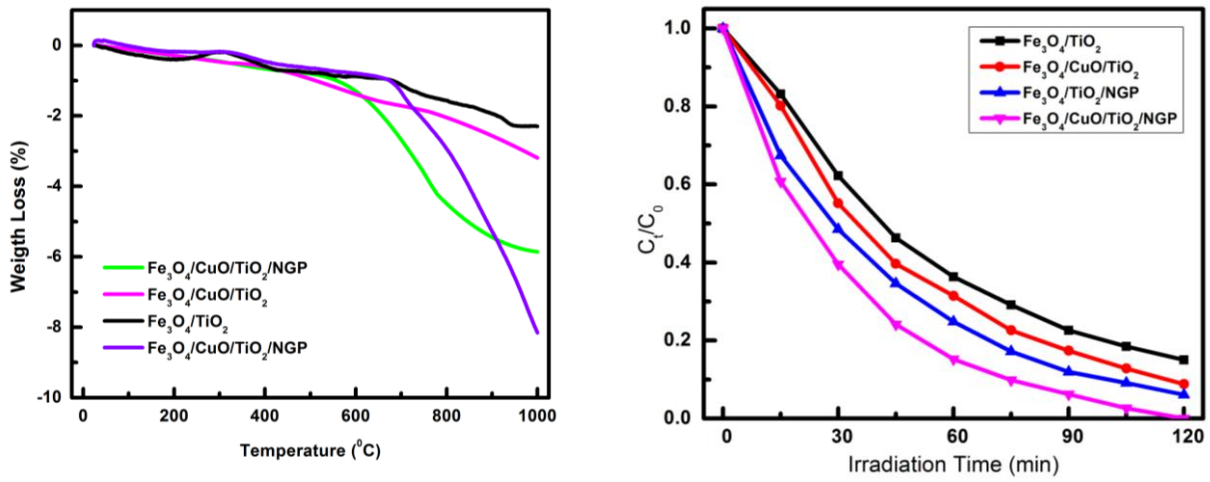

Figure 2. (a) TGA pattern of Fe_3O_4/TiO_2, $Fe_3O_4/CuO/TiO_2$, $Fe_3O_4/TiO_2/NGP$ and $Fe_3O_4/CuO/TiO_2/NGP$ nanocomposites, **(b)** Degradation efficiency of Fe_3O_4/TiO_2, $Fe_3O_4/CuO/TiO_2$, $Fe_3O_4/TiO_2/NGP$ and $Fe_3O_4/CuO/TiO_2/NGP$ nanocomposites under combination of UV light and ultrasonic irradiation.

Figure 2(b) shows the decolorization process of MB with photosonocatalytic by using Fe_3O_4/TiO_2, $Fe_3O_4/TiO_2/NGP$, $Fe_3O_4/CuO/TiO_2$, and $Fe_3O_4/CuO/TiO_2/NGP$ catalysts with dosage 0.2 g/L. The curves in the figure show that the presence of NGP can improve photosonocatalytic performance of both Fe_3O_4/TiO_2 and $Fe_3O_4/CuO/TiO_2$ nanocomposites. This may be due to the ability of NGP to inhibit the recombination rate of electron and hole since graphene can act as an electron acceptor in the photosonocatalytic reaction [22]. In addition, it can also be seen that the addition of CuO on both Fe_3O_4/TiO_2 nanocomposites with and without NGP improve the performance of both catalyst to degrade MB. Photosonocatalytic performance increase with the presence of CuO due to the formation of heterojunction on TiO_2 coupling with CuO can inhibit recombination of electron and hole [23].

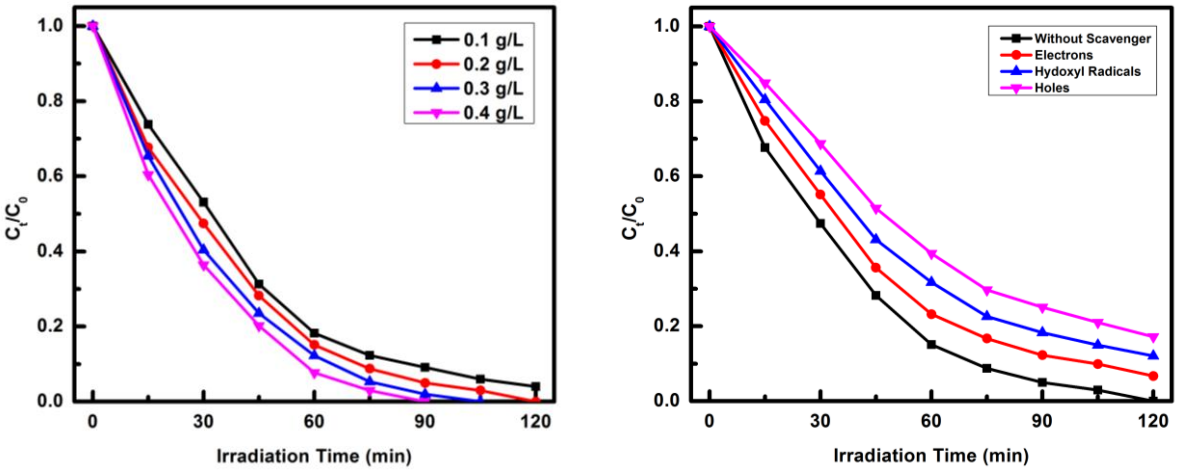

Figure 3. (a) Influence of dosage catalyst and **(b)** Effect of different Scavengers on catalytic activity of $Fe_3O_4/CuO/TiO_2/NGP$.

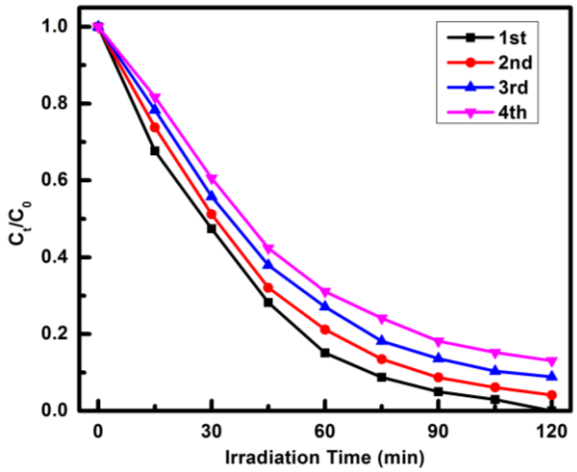

Figure 4. Influence of reusability of catalyst

Photosonocatalytic process in degrading MB for four dosages of the $Fe_3O_4/CuO/TiO_2/NGP$ nanocomposites are shown in Figure 3(a). The result shows that the dosage of 0.4 g/L indicates the best photosonocatalytic performance in degrading MB reaches 100% within 90 minutes. Increasing dosage of the catalyst is expected to enlarge the surface area involved in the process [24]. Moreover, the addition of dosage may also increase the formation of electrons and holes that can affect the amount of hydroxyl radicals and superoxide, [24] hence can break the MB molecules.

To examine the species that play an active role in the process of MB degradation, the scavenger materials are added into MB solution to detect the main species that contribute to the photosonocatalytic process. The scavenger materials used are among others tert-butyl alcohol, ammonium oxalate and $Na_2S_2O_8$ each of which plays the role as hydroxyl radicals , holes , and electrons respectively. There are shown in Figure 3(b). The addition of ammonium oxalate scavenger indicates lowest photosonocatalytic activities. It can be seen that ammonium oxalate provoke a large degree of inhibition of MB, which confirmed the indispensable role of holes in the degradation process of MB.

To examine the stability of $Fe_3O_4/CuO/TiO_2/NGP$ in photosonocatalytic process, the catalyst is reused four times cycling processes and the results of each performance are shown in Figure 4. $Fe_3O_4/CuO/TiO_2/NGP$ catalyst still showed good performance after reuse fourth time and only a slight decline of about 8 % in MB degradation. Decline in catalyst performance is suspected because of its lost when the catalyst is separated from its solution to be reuse. This result proves that the Fe_3O_4/TiO_2 nanocomposites with the presence of CuO and NGP simultaneously has the potential to be used as catalyst to degrade organic dye waste.

4. Conclusion

The presence of CuO and NGP in Fe_3O_4/TiO_2 nanocomposites that have been successfully synthesized using the method of co-precipitation are able to improve the *photosonocatalysis* performance to degrade the organic dye waste methylene blue until 100% by inhibiting recombination rate of electrons and holes in synergy with enlarging their surface areas, and do not reduce much on their potential for reuse.

References

[1] Zhang H,Wei C, Huang Y, Wang J 2016 *Ultrasonics Sonochemistry* **30** 61–69
[2] Salem IA, El-Maazawi MS 2000 *Chemosphere* **41** 1173–118
[3] Fung PC, Huang Q, Tsui SM, Poon CS 1999 *Water Science and Technology* **40** 153-160.
[4] Wang J, Ma T, Zhang ZH, Zhang XD, Jiang YF, Zhang G, Zhao G, Zhao HD, Zhang P 2007 *Ultrasonics Sonochemistry*, **14** 246–252

[5] Suslick KS, Doktycz SJ, Flint EB 1990 *Ultrasonics* **28** 280–290.
[6] Sathishkumar P, Mangalaraja RV, Mansilla HD, Pinilla MAG, Anandan S 2014 *Applied Catalysis B: Environmental* **160–161** 692–700.
[7] Tangestaninejad S, Moghadam M, Mirkhani V, Baltork IM, Salavati H 2008 *Ultrasonics Sonochemistry* **15** 815–822
[8] Khan MAN, Siddique M, Wahid F, Khan R 2015 *Ultrasonics Sonochemistry* **26** 370–377
[9] Reddy DR, Dinesh GK, Anandan S, Sivasankar T, 2016 *Chemical Engineering and Processing* **99** 10–18
[10] Ertugay N, Acar FN 2014 *Applied Surface Science* **318** 121–126
[11] Wang H, Niu J, Long X, He Y, (2008) *Ultrasonics Sonochemistry* **15** 386–392
[12] Li D, Wang J, Li X, Liu H 2012 *Materials Science in Semiconductor Processing* **15** 152–158
[13] Ahmad M, Ahmed E, Hong ZL, Ahmed W, Elhissi A, Khalid NR 2014 *Ultrasonics Sonochemistry* **21** 761–773
[14] Abbas M, Rao BP, Reddy V, Kim C 2014 *Ceramics International* **40** 11177–11186
[15] Samad A, Furukawa M, Katsumata H, Suzuki T, Kaneco S 2016 *Journal of Photochemistry and Photobiology A: Chemistry* **325** 97–103
[16] Liu Z, Bai H, Xu S, Sun DD, (2011) *International journal of hydrogen energy* **36** 13473-13480
[17] Subhan MA, Uddin N, Sarker P, Azad AK, Begum K 2015 *Spectrochimica Acta Part A: Molecular and Biomolecular Spectroscopy* **149** 839–850
[18] Fan C, Liu Q, Ma T, Shen J, Yang Y, Tang H, Wang Y, Yang J 2016 *Ceramics International* **42** 10487–10492
[19] Li Y, Zhang Z, Pei L, Li X, Fan T, Ji J, Shen J, Ye M 2016 *Applied Catalysis B: Environmental* **190** 1–11
[20] Arifin SA, Jalaludin S, and Saleh R 2015 *Materials Science Forum* **827** 49-55
[21] Heidari EK, et al. 2015 *Journal of Magnetism and Magnetic Materials*, **379** 7906-7915
[22] Vinothkannan M, Karthikeyan C, Kumar GG, Kim AR, Yoo DJ 2015 *Spectrochimica Acta Part A: Molecular and Biomolecular Spectroscopy*, **135** 256-264
[23] Qin S, Xin F, Liu Y, Yin X and Ma W 2011 *Journal of Colloid and Interface Science* **357** 257-261,
[24] Saleh R and Djaja N, 2014.*Superlattices and Microstructures* **74** 217-233,